Electronic Supplementary Material

Metal phosphonate-derived cobalt/nickel phosphide@N-doped carbon hybrids as efficient bifunctional oxygen electrodes for Zn-air batteries

Cai-Yue Wang*, Meng-Qi Gao*, Cheng-Cai Zhao, Li-Min Zhao, Hui Zhao (✉)
School of Materials Science and Engineering, Liaocheng University, Liaocheng 252000, Shandong, China
E-mail: zhaohui@lcu.edu.cn

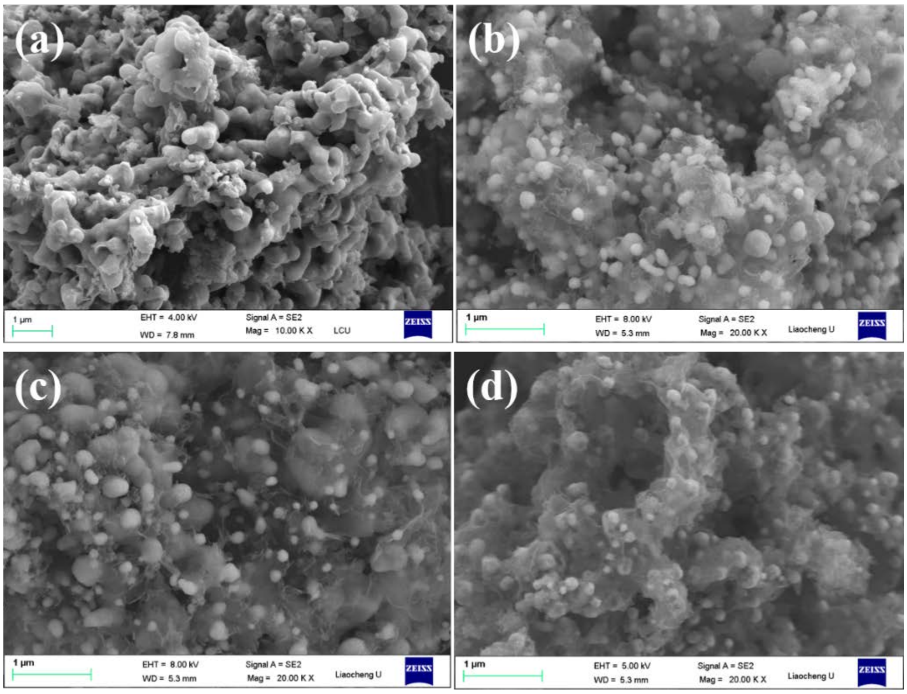

Fig. S1. FESEM image of the as-synthesized Co_2P@NC (a), Co_2P/Ni_3P@NC-0.2 (b), Co_2P/Ni_3P@NC-0.5 (c), Co_2P/Ni_3P@NC-0.2 (d).

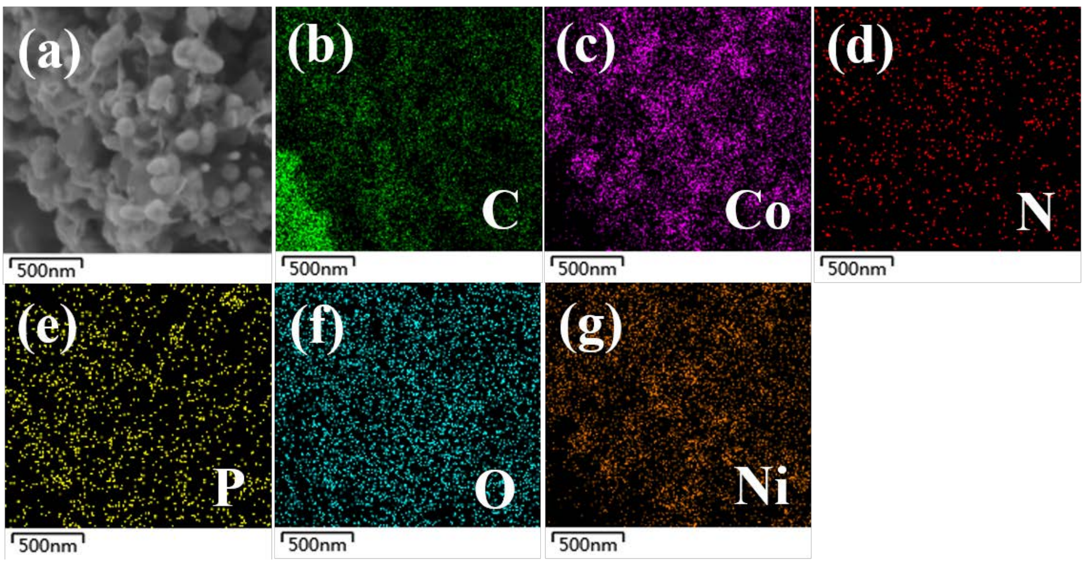

Fig. S2. FESEM image (a) and EDS elemental mapping images (b-g) of the Co_2P/Ni_3P@NC-0.2.

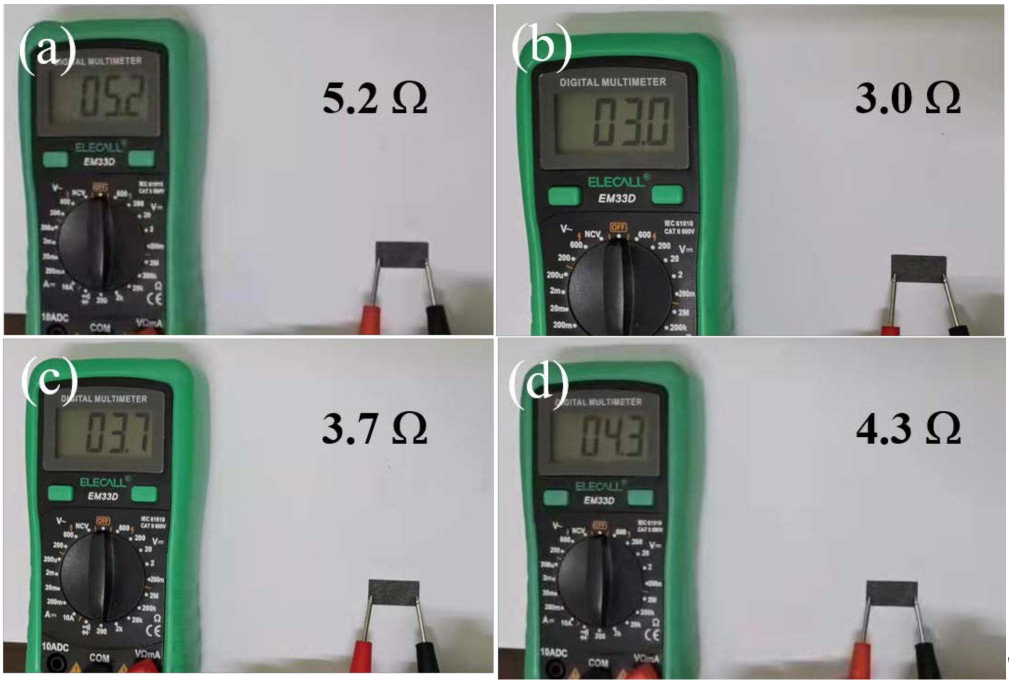

Fig. S3. Resistance tests of catalysts.

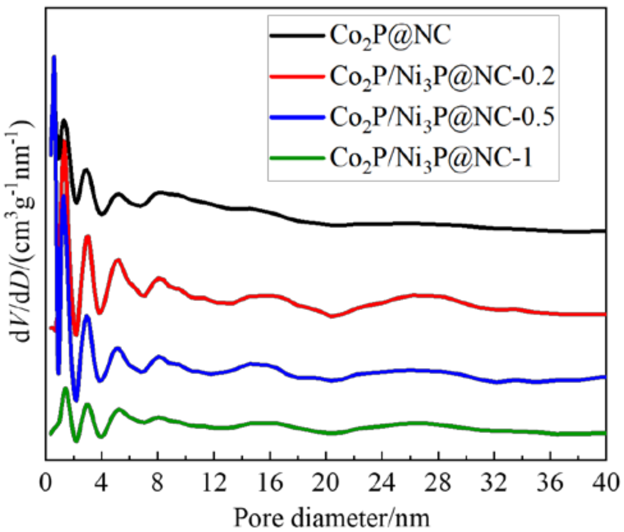

Fig. S4. Pore size distributions of the as-synthesized samples.

The XPS fitting standard is as follows. First, for the p, d and f levels, the intensity ratio of their sub levels (such as $P_{3/2}$ and $P_{1/2}$) is certain ($P_{3/2}$: $P_{1/2}$ = 2:1). Second, for the energy levels (p, d, f) with energy level splitting, the distance between the two orbitals is basically fixed. Third, for the splitting orbits of the same element, the half peak width should be as close as possible.

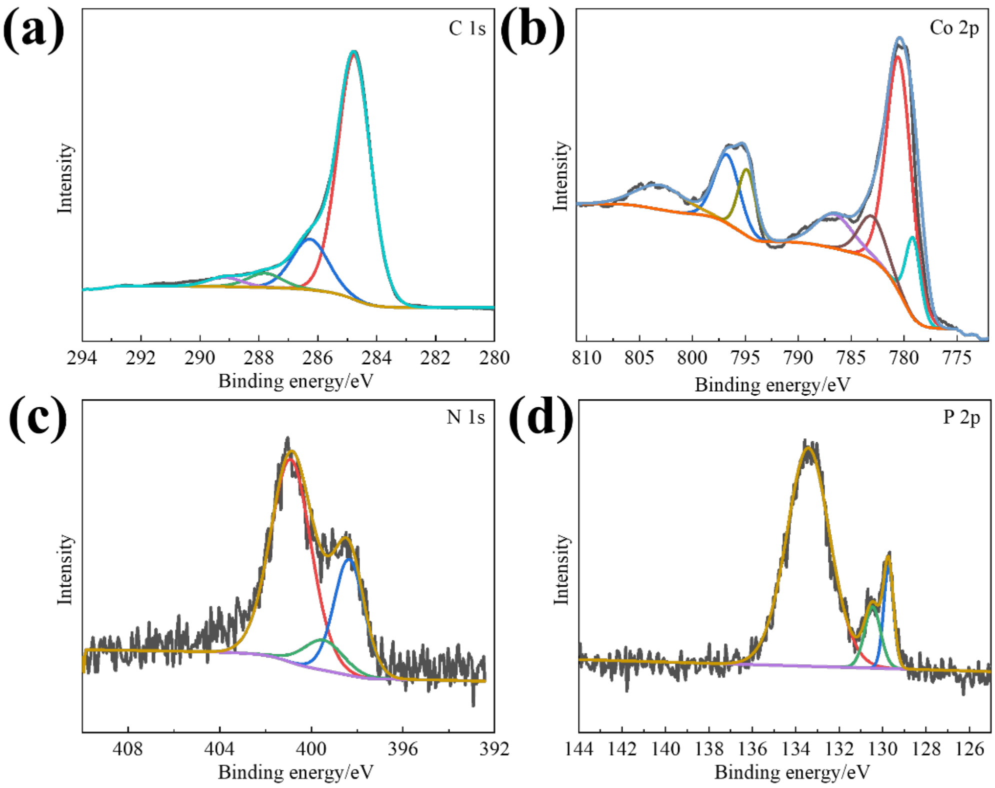

Fig. S5. High-resolution XPS spectra of C 1s (a), Co 2p (b), N 1s (c) and P 2p (d) of Co_2P@NC catalyst.

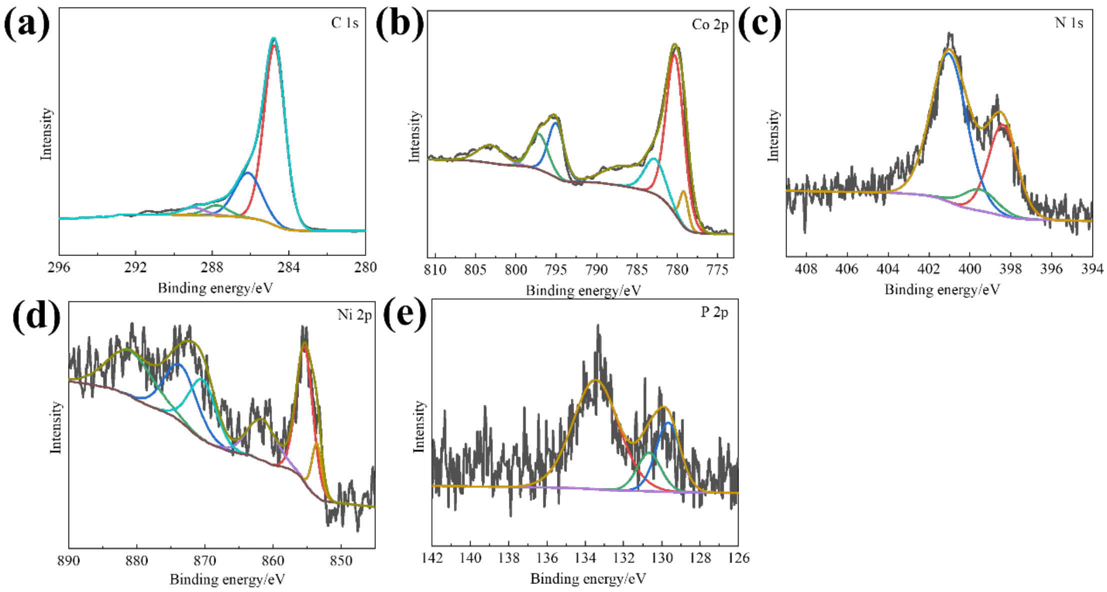

Fig. S6. High-resolution XPS spectra of C 1s (a), Co 2p (b), N 1s (c), Ni 2p (d) and P 2p (e) of Co_2P/Ni_3P@NC-0.5 catalyst.

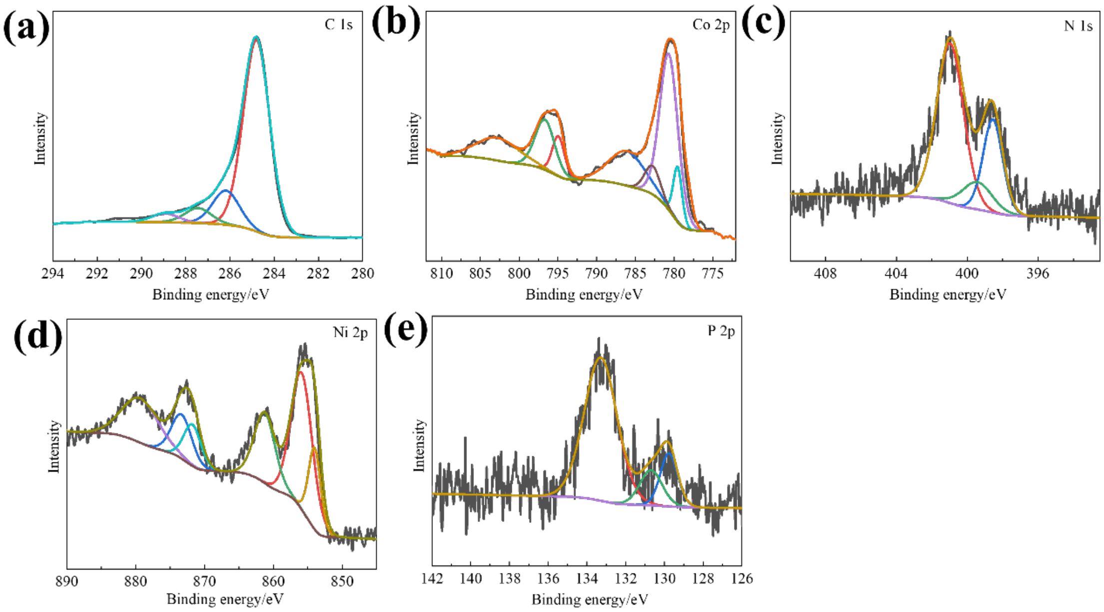

Fig. S7. High-resolution XPS spectra of C 1s (a), Co 2p (b), N 1s (c), Ni 2p (d) and P 2p (e) of Co_2P/Ni_3P@NC-1 catalyst.

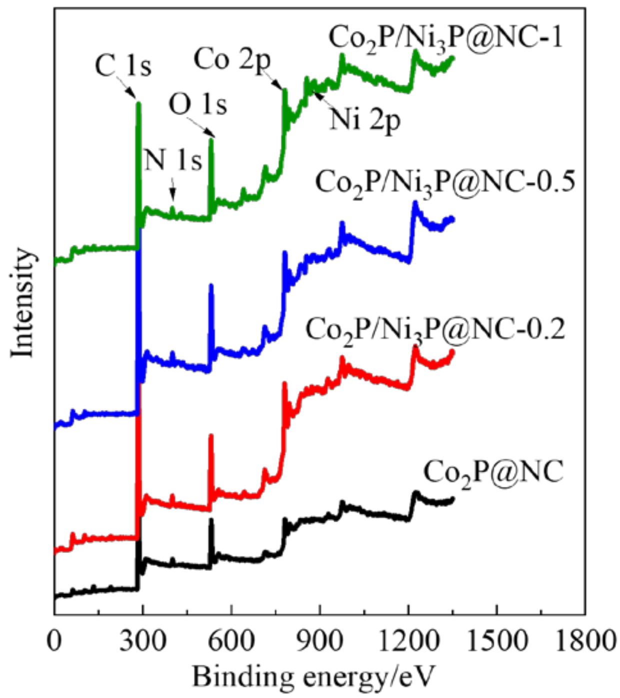

Fig. S8. XPS survey spectra of the as-synthesized samples.

Table S1. The total contents of C, O, N, Co, Ni and P of catalysts.

catalyst	C (at.%)	O (at.%)	N (at.%)	Co (at.%)	Ni (at.%)	P (at.%)
Co_2P @NC	74.37	13.69	4.19	4.71	0	3.03
Co_2P/Ni_3P@NC-0.2	74.22	14.16	4.37	4.45	0.97	1.84
Co_2P/Ni_3P@NC-0.5	75.17	13.27	4.7	3.82	1.23	1.82
Co_2P/Ni_3P@NC-1	72.59	14.6	4.4	3.90	2.76	1.75

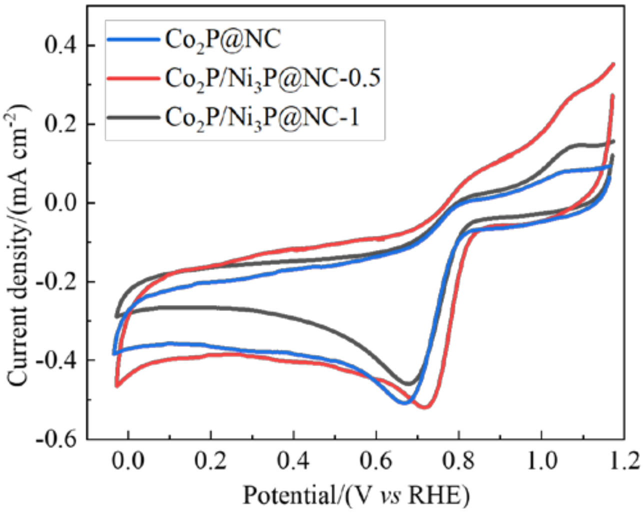

Fig. S9. CV curves of Co_2P@NC, Co_2P/Ni_3P@NC-0.5 and Co_2P/Ni_3P@NC-1.

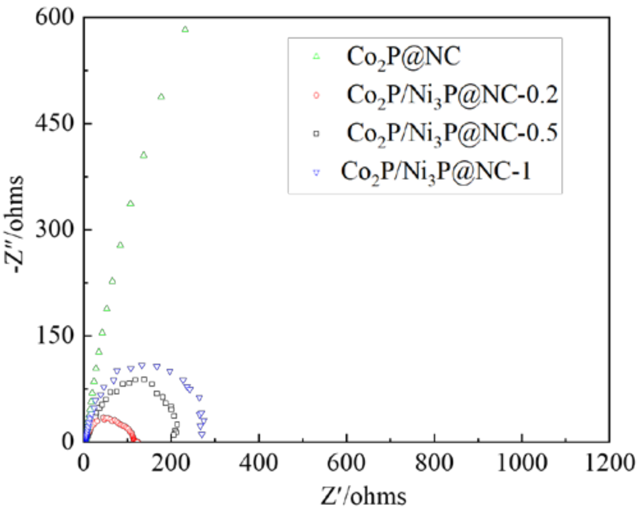

Fig. S10. EIS of fabricated catalysts for OER in O_2-saturated 0.1M KOH.

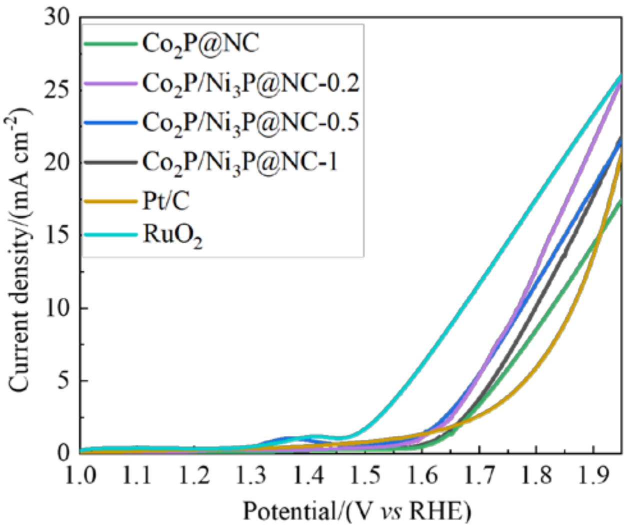

Fig. S11. LSV curves of fabricated catalysts for OER in O_2-saturated 0.1M KOH.

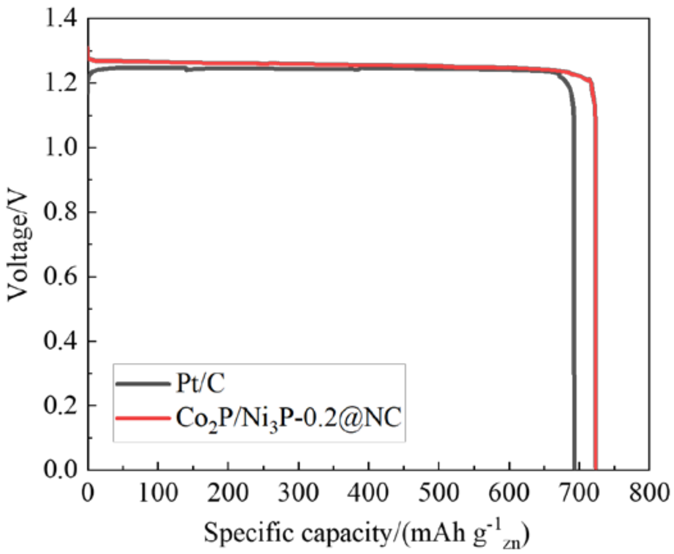

Fig. S12. Specific capacity of the Co_2P/Ni_3P@NC-0.2 and Pt/C-based Zn-air batteries.

Table S2. Comparison of ORR catalytic performances between Co_2P/Ni_3P@NC-0.2 and previously reported transition metal-based materials.

Catalyst	Catalyst loading (mg cm^{-2})	Electrolyte	Onset potential (V, vs.RHE)	Half-wave potential (V, vs.RHE)	Electron transfer number (*n*)	Reference
Co_2P/Ni_3P@NC-0.2	0.255	0.1M KOH	0.90	0.80	3.91	This work
CoP/CN/Ni	0.41	0.1M KOH		0.80	3.6~3.8	1
Fe–NiCoP@C	1.64	0.1M KOH	0.81		3.75	2
Co@WC_{1-x}/NCNT	0.56	0.1M KOH	0.91	0.81	3.89	3
Co_2P/CoNPC	0.255	0.1M KOH	0.963	0.843	3.87	4
Co/SiO_2/N-C (900)	0.46	0.1M KOH	0.90	0.81	3.78	5
MnO/Co/PGC	0.51	0.1M KOH	0.95	0.78	N.A.	6

Table S3. Comparison of the primary Zn-air batteries for several recently reported highly active transition metal–based catalysts.

Catalyst	Electrolyte	Open circuit voltage (V)	Peak power density (mW	Charge-discharge current density (mA cm^{-2})	Cycling tests	Ref.

			cm^{-2})			
Co_2P/Ni_3P@NC-0.2	6M KOH	1.386	95	10	249 cycles; 166 h	This work
CoP	6M KOH	1.34	61	10		7
Co/SiO_2/N-C	6M KOH	1.41	138.2	5	600 cycles; 400 h	5
CoP_x@CNS	6M KOH	1.40	110	5	400 cycles; 130 h	8
CoO-NSC-900	6M KOH	1.4	~67	10	60 h	9
Al, P-codoped Co_3O_4/NF	6M KOH	1.436	89.1	10	150 cycles; 3000 min	10
FeNi@N-CNT/NCS	6M KOH	1.49	103	10	120 cycles; 40 h	11

References:

1. Chen T, Ma J, Chen S Y, Wei Y M, Deng C S, Chen J C, Hu J Q, Ding W P. Construction of heterostructured CoP/CN/Ni: Electron redistribution towards effective hydrogen generation and oxygen reduction. Chemical Engineering Journal, 2021, 415: 129031

2. Kang Y, Wang S, Zhu S Q, Gao H X, Hui K S, Yuan C Z, Yin H, Bin F, Wu X L, Mai W J, et al. Iron-modulated nickel cobalt phosphide embedded in carbon to boost power density of hybrid sodium–air battery. Applied Catalysis B: Environmental, 2021, 285: 119786

3. Cai J N, Zhang X F, Yang M X, Shi Y D, Liu W K, Lin S. Constructing Co@WC_{1-x} heterostructure on N-doped carbon nanotubes as an efficient bifunctional electrocatalyst for zinc-air batteries Journal of power sources, 2021, 485: 229251

4. Liu H T, Guan J Y, Yang S X, Yu Y H, Shao R, Zhang Z P, Dou M L, Wang F, Xu Q. Metal–organic-framework-derived Co_2P nanoparticle/multi-doped porous carbon as a trifunctional electrocatalyst. Advanced Materials, 2020, 32(36): 2003649

5. Guo X T, Zheng S S, Luo Y Q, Pang H. Synthesis of confining cobalt nanoparticles within SiO_x/nitrogen-doped carbon framework derived from sustainable bamboo leaves as oxygen electrocatalysts for rechargeable Zn-air batteries, Chemical Engineering Journal, 2020, 401: 126005

6. Lu X F, Chen Y, Wang S B, Gao S Y, Lou X W. Interfacing manganese oxide and cobalt in porous graphitic carbon polyhedrons boosts oxygen electrocatalysis for Zn–air batteries. Advanced Materials, 2019, 31(39): 1902339

7. Li H, Li Q, Wen P, Williams T B, Adhikari S, Dun C C, Lu C, Itanze D, Jiang L, D L Carroll. et al. Colloidal cobalt phosphide nanocrystals as trifunctional electrocatalysts for overall water splitting powered by a zinc–air battery. Advanced Materials, 2018, 30(9): 1705796

8. Hou C C, Zou L L, Wang Y, Xu Q. MOF-mediated fabrication of a porous 3D superstructure of carbon nanosheets decorated with ultrafine cobalt phosphide nanoparticles for efficient electrocatalysis and zinc–air batteries. Angewandte Chemie International Edition, 2020, 132(48): 21544–21550

9. Chen S, Chen S, Zhang B H, Zhang J T. Bifunctional oxygen electrocatalysis of N, S-codoped porous carbon with interspersed hollow CoO nanoparticles for rechargeable Zn−air batteries. ACS Applied Materials & Interfaces, 2019, 11(18): 16720–16728
10. Lv X W, Liu Y P, Tian W W, Gao L J, Yuan Z Y. Aluminum and phosphorus codoped “superaerophobic”Co_3O_4 microspheres for highly efficient electrochemical water splitting and Zn-air batteries. Journal of Energy Chemistry, 2020, 50: 324–331
11. Ren J T, Chen L, Wang Y S, Tian W W, Gao L J, Yuan Z Y FeNi nanoalloys encapsulated in N-doped CNTs tangled with N-doped carbon nanosheets as efficient multifunctional catalysts for overall water splitting and rechargeable Zn−air batteries. ACS sustainable Chemistry & Engineering, 2020, 8(1): 223–237